NASA/TM—2010-216074 AIAA–2009–5117

Shock Positioning Controls Design for a Supersonic Inlet

George Kopasakis and Joseph W. Connolly
Glenn Research Center, Cleveland, Ohio

February 2010

NASA STI Program . . . in Profile

Since its founding, NASA has been dedicated to the advancement of aeronautics and space science. The NASA Scientific and Technical Information (STI) program plays a key part in helping NASA maintain this important role.

The NASA STI Program operates under the auspices of the Agency Chief Information Officer. It collects, organizes, provides for archiving, and disseminates NASA's STI. The NASA STI program provides access to the NASA Aeronautics and Space Database and its public interface, the NASA Technical Reports Server, thus providing one of the largest collections of aeronautical and space science STI in the world. Results are published in both non-NASA channels and by NASA in the NASA STI Report Series, which includes the following report types:

- TECHNICAL PUBLICATION. Reports of completed research or a major significant phase of research that present the results of NASA programs and include extensive data or theoretical analysis. Includes compilations of significant scientific and technical data and information deemed to be of continuing reference value. NASA counterpart of peer-reviewed formal professional papers but has less stringent limitations on manuscript length and extent of graphic presentations.

- TECHNICAL MEMORANDUM. Scientific and technical findings that are preliminary or of specialized interest, e.g., quick release reports, working papers, and bibliographies that contain minimal annotation. Does not contain extensive analysis.

- CONTRACTOR REPORT. Scientific and technical findings by NASA-sponsored contractors and grantees.

- CONFERENCE PUBLICATION. Collected papers from scientific and technical conferences, symposia, seminars, or other meetings sponsored or cosponsored by NASA.

- SPECIAL PUBLICATION. Scientific, technical, or historical information from NASA programs, projects, and missions, often concerned with subjects having substantial public interest.

- TECHNICAL TRANSLATION. English-language translations of foreign scientific and technical material pertinent to NASA's mission.

Specialized services also include creating custom thesauri, building customized databases, organizing and publishing research results.

For more information about the NASA STI program, see the following:

- Access the NASA STI program home page at *http://www.sti.nasa.gov*

- E-mail your question via the Internet to *help@sti.nasa.gov*

- Fax your question to the NASA STI Help Desk at 443–757–5803

- Telephone the NASA STI Help Desk at 443–757–5802

- Write to:
  NASA Center for AeroSpace Information (CASI)
  7115 Standard Drive
  Hanover, MD 21076–1320

NASA/TM—2010-216074 AIAA–2009–5117

Shock Positioning Controls Design for a Supersonic Inlet

George Kopasakis and Joseph W. Connolly
Glenn Research Center, Cleveland, Ohio

Prepared for the
45th Joint Propulsion Conference and Exhibit
cosponsored by the AIAA, ASME, SAE, and ASEE
Denver, Colorado, August 2–5, 2009

National Aeronautics and
Space Administration

Glenn Research Center
Cleveland, Ohio 44135

February 2010

Acknowledgments

The authors would like to express their gratitude to the Supersonics Project of the NASA Fundamental Aeronautics Program for supporting this research effort.

This report contains preliminary findings, subject to revision as analysis proceeds.

This work was sponsored by the Fundamental Aeronautics Program at the NASA Glenn Research Center.

Level of Review: This material has been technically reviewed by technical management.

Available from

NASA Center for Aerospace Information
7115 Standard Drive
Hanover, MD 21076–1320

National Technical Information Service
5301 Shawnee Road
Alexandria, VA 22312

Available electronically at http://gltrs.grc.nasa.gov

Shock Positioning Controls Design for a Supersonic Inlet

George Kopasakis and Joseph W. Connolly
National Aeronautics and Space Administration
Glenn Research Center
Cleveland, Ohio 44135

Abstract

Under the NASA Fundamental Aeronautics Program, the Supersonics Project is working to overcome the obstacles to supersonic commercial flight. The supersonic inlet design that is utilized to efficiently compress the incoming air and deliver it to the engine has many design challenges. Among those challenges is the shock positioning of internal compression inlets, which requires active control in order to maintain performance and to prevent inlet unstarts due to upstream (freestream) and downstream (engine) disturbances. In this paper a novel feedback control technique is presented, which emphasizes disturbance attenuation among other control performance criteria, while it ties the speed of the actuation system(s) to the design of the controller. In this design, the desired performance specifications for the overall control system are used to design the closed loop gain of the feedback controller and then, knowing the transfer function of the plant, the controller is calculated to achieve this performance. The innovation is that this design procedure is methodical and allows maximization of the performance of the designed control system with respect to actuator rates, while the stability of the calculated controller is guaranteed.

I. Introduction

The supersonic inlet compresses incoming air supersonically and through the subsonic diffuser, in the process forming an oblique shock system and a normal shock in the vicinity where the flow changes from supersonic to subsonic, as shown for an axisymmetric inlet in Figure 1. If the normal shock travels slightly upstream of the throat area, the shock is quickly expelled from the inlet causing the inlet to unstart and creating large frictional forces in front of the inlet. On the other hand, if the normal shock is ingested by the engine that can result in component damage. Therefore, the normal shock position needs to be controlled at some distance downstream of the throat restriction to prevent such undesirable effects. However, propulsion efficiency increases as the shock position is controlled closer to this throat restriction, and thus a good control design that rejects disturbances can reduce this shock position margin and improve propulsion efficiency.

Traditionally, proportional or proportional integral (PI) type control designs have been employed for inlet shock positioning control systems (Refs. 1 and 2). Predictive and optimal controls combined with PI are used in References 3 to 5. Quadratic Optimization is used in Reference 6 to minimize the expected frequency of inlet unstarts. These designs, however, do not take advantage of actuator speeds or bandwidths to maximize disturbance rejection, while maintaining desirable control system performance. The controls design that will be discussed in this paper is based on the loop shaping technique discussed in Reference 7, which shapes the closed loop gain of the system based on the actuator speeds, for disturbance rejection and stability performance criteria. This feedback control design technique is systematic, and allows for a control design that maximizes performance with respect to the speed of the plant and its actuation system(s). Even though satisfactory control may be achieved without a systematic design technique, there could be a sacrifice in shock position margin, which impacts the pressure recovery and thus, the inlet efficiency.

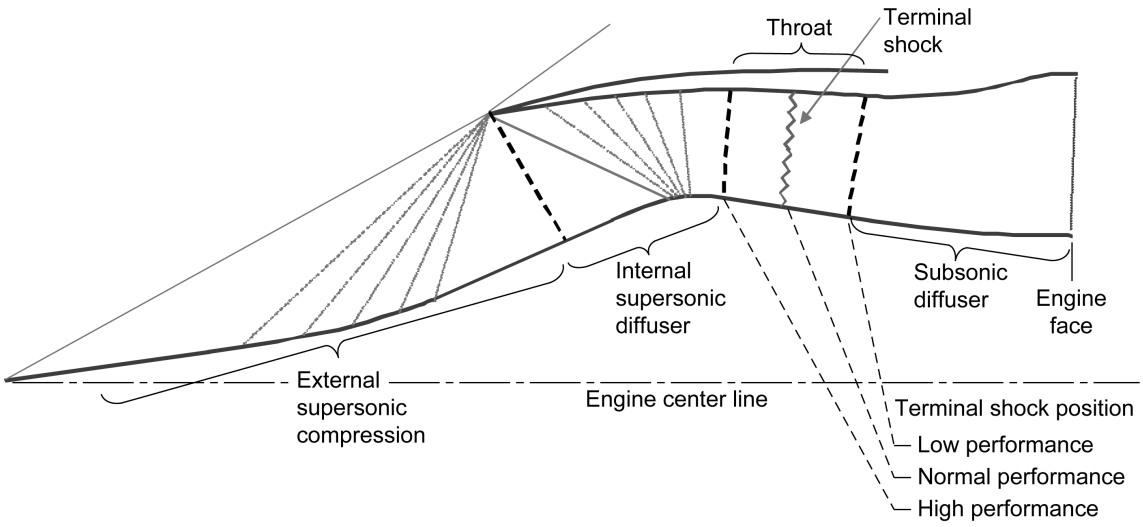

Figure 1.—Centerline diagram of a supersonic axisymmetric inlet with translating and collapsing centerbody.

A nonlinear inlet model named LAPIN (Large Perturbations Inlet) was utilized and perturbed to develop plant transfer functions (TF) for controls design. This inlet model is a quasi-1–D model based on the method of characteristics, developed at NASA Glenn Research Center (Ref. 8). This model allows for geometry manipulations and can be used to develop simulations of internal compression inlets of different geometries.

The loop shaping feedback control design for inlet shock positioning follows the approach described in Reference 7. In this approach, the closed loop gain of the system is designed in the frequency domain to achieve maximum disturbance attenuation within the capability of the actuation system, while at the same time maintaining adequate gain and phase margins, as well as other performance criteria such as response and settling times. Then, knowing the TF of the plant, the plant is subtracted from the overall closed loop gain (in dB scale) which gives the desired feedback controller TF. The resulting controller TF is then fitted with poles and zeros in order to calculate the controller that will achieve the desired closed loop gain that meets the feedback control system performance requirements. The whole control design process is methodical, and also demonstrates how to trade between conflicting performance criteria. The innovation in the technique lies in its ability to directly tie actuator rates to the maximum performance attainable in the controls design. Also, by following the approach in Reference 7 of fitting the controller TF (magnitude and phase) with poles and zeros, explicit plant inversion is avoided, which guarantees stable controllers.

Based on this approach, first the feedback controls of the bypass door actuation system utilized for the shock control is designed to have high bandwidth with high disturbance attenuation and adequate stability margins. This is followed by the feedback design of the shock positioning controls themselves in the presence of atmospheric disturbances, as covered in Reference 9.

The paper is organized as follows. First, the feedback control systems loop shaping design approach (Ref. 7) is described, followed by a description of the linear inlet model derived by perturbing the nonlinear LAPIN model. Next, the bypass door actuator model and its feedback control design are described, followed by a description of atmospheric disturbances. Then the design of the shock position controller is covered, followed by a description of its performance attenuating atmospheric disturbances. Finally, some concluding remarks are presented.

II. Feedback Control Systems Loop Shaping Design Methodology

In this section a brief description of the loop shaping design methodology will be given. For more detail on this approach the reader is referred to Reference 7. This loop shaping design methodology is a systematic feedback controls systems approach, which is designed to simultaneously meet a variety of control performance criteria or specifications. The approach is to design the overall closed loop gain of the control system based on the performance criteria and the speed of the actuation system first. This is followed by designing the controller so that the closed loop system meets the desired closed loop gain. This is accomplished with an emphasis on maximizing disturbance rejection while meeting adequate stability margins, emphasizing how to trade-off these competing requirements.

A traditional feedback control system diagram is shown in Figure 2, with the controller the plant and disturbance TFs shown as G_c, G_p, and G_d respectively. The closed loop gain (CLG) is defined as the product of the TFs in the closed loop system, which includes the feedback. For distinction, the CLG is the gain that appears in the denominator of a feedback control system TF. Whereas, the open loop gain is the gain that appears in the numerator of that TF, with those gains being the same when the feedback gain is unity. Thus, for unity feedback, as will be the case for the shock position control design presented, the CLG of the control system is

$$L(s) = G_c(s)G_p(s) \tag{1}$$

It is this CLG that is shaped in this approach based on the design criteria or requirements. The first step is to choose the maximum bandwidth of the feedback control system. This translates to how fast the system can be driven without saturation or damage to the hardware. From Reference 7, the crossover frequency or the bandwidth of the control system (i.e., the frequency where the CLG crosses the 0 dB axis) in rad/s, can be computed as

$$\omega_{co} = C_r \, a_{rl} / r_m \tag{2}$$

where r_m is the maximum step input of the system, a_{rl} is actuator rate limit in units of magnitude per second, and C_r is the ratio of system output response to actuator input. Typically, for a unit step input and for C_r=1, the cross-over frequency is equal to the actuation rate limit. The cross over frequency of the CLG, ω_{co}, is also associated with the response or time constant of the system (i.e., the time at which the time response reaches 63 percent of its final value) as τ_{tc}=1/ ω_{co}. The input to output frequency response of the control system can be expressed as

$$\frac{C(s)}{R(s)} = \frac{L(s)}{1+L(s)} \tag{3}$$

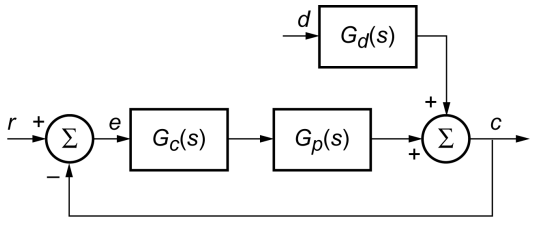

Figure 2.—Feedback control system diagram.

The disturbance response TF, for disturbance coming in at the plant output, can be expressed as

$$\frac{C(s)}{D(s)} = \frac{G_d(s)}{1 + L(s)} \tag{4}$$

From Equation (3) it can be seen that the CLG is directly associated with the stability characteristics of the closed loop system and from Equation (4) it can be seen that the CLG is also directly associated with the ability of the system to reject disturbances. Since, the time constant(s) of the system are also a part of the CLG, designing for the CLG addresses all the requirements associated with the performance of classical feedback control systems.

Figure 3 shows an example CLG design, with the associated time response of the closed loop system shown in Figure 4, based on the following CLG transfer function

$$L(s) = 353.13 \frac{(s/25 + 1)}{s(s/100 + 1)(s/1000 + 1)} \tag{5}$$

In Figure 3 the symbol *DA* signifies disturbance attenuation at the mid-frequency band, and ϕM signifies phase margin for stability. Closed loop gain designs can be easily realized based on the control system performance requirements, following the process described in Reference 7. In this design the gain margin is infinite and it is not shown. The gain margin is the difference in gain between the 0 dB and the gain at the frequency at which the phase crosses –180°. In this design the closed loop system has two dominant time constants; the initial time constant that is related to the cross-over frequency as discussed before and associated with the fast second order type response, followed by a time constant associated with the frequency of the zero in Equation (5) with a first order response. These time constants are evident in the response of Figure 4; first the initial rapid underdamped response, followed by the longer response before the system settles. The inset in Figure 4 shows a longer time response at the neighborhood of the amplitude that is dominated by the first order response of the zero. The advantages of these two time constants or dominant natural responses together in the design are increased disturbance attenuation and enhanced stability (Ref. 7), as will be discussed later.

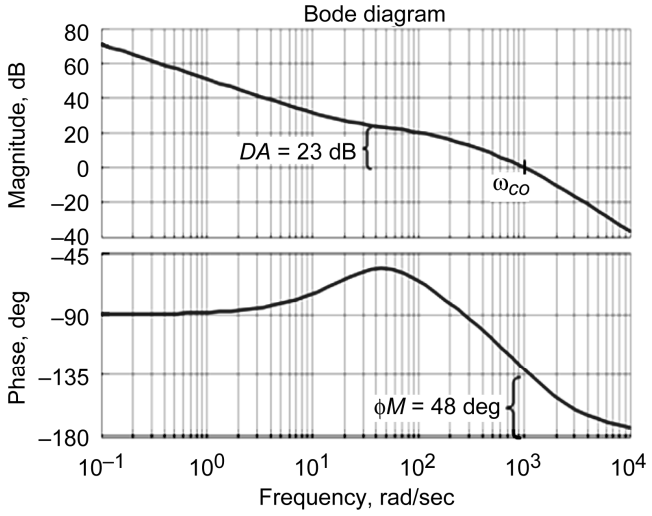

Figure 3.—Example of CLG design.

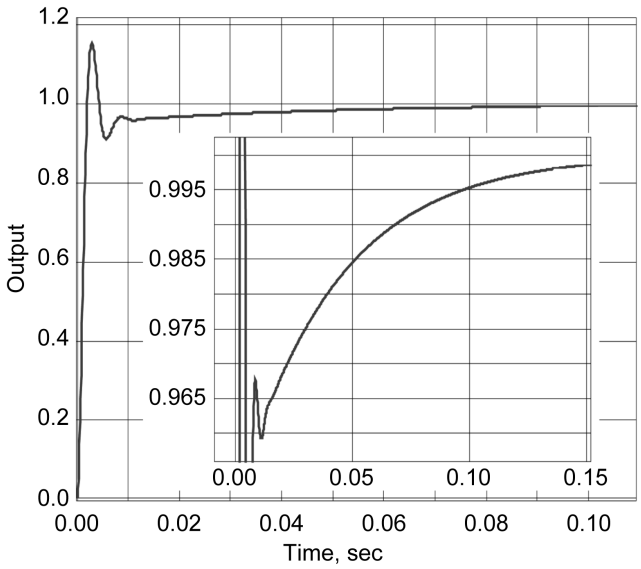

Figure 4.—Step response.

In brief, the design of the CLG starts with deciding on the bandwidth or the cross-over frequency based on Equation (2). This is followed by placing a pole at the origin for zero steady-state error, a zero at some low frequency to boost the phase for stability and for high disturbance attenuation at the mid-frequency range as well as for settling time requirements (not all of these objectives are in concert), followed by a pole at approximately one decade below the desired cross-over frequency. Typically, such a design with two poles and one zero can be made to achieve approximately 20 dB disturbance attenuation at the mid-frequency range, up to one decade before the cross-over frequency. Designing for 20 dB disturbance attenuation at the mid-frequency range is near the maximum achievable considering the actuator bandwidth. Slightly more disturbance attenuation is possible, however, in that case the design of the CLG would end up being higher order and trade the stability margins for disturbance attenuation, as evident with the CLG example in Figure 3.

Following the design of the CLG based on the feedback control system performance requirements, the process TF is subtracted from the designed CLG in the frequency domain (dB scale) to come-up with the controller design frequency response. This frequency response is then fitted with poles and zeros as detailed in Reference 7, in order to come-up with the controller design. As a final step, the designed CLG based on the specification is compared to the actual CLG obtained from this design process. Since the publishing of Reference 7, the process of calculating the controller frequency response was automated, by forming the complex vectors of the CLG and the process TFs and subtracting these vectors in dB scale to come up with the controller frequency response. The last step of fitting the controller TF with poles and zeros is still being performed manually, following the process outlined in Reference 7.

III. Linear Supersonic Inlet Model

For the supersonic inlet model, LAPIN was utilized, which simulates a finite quasi 1–D internal compression inlet, utilizing a modeling methodology associated with the method of characteristics. This model also includes upstream volume elements starting from the freestream and thus, it includes a representative simulation of oblique shock(s) bouncing off the inlet forebody. The accuracy of this model has been verified against experimental data obtained for internal compression inlets (Ref. 8). This simulation allows the user to define the inlet geometry in the 1–D sense. Since the emphasis of the NASA Supersonics Project is fundamental research, the project hasn't baselined an inlet geometry. Thus, the two-dimensional bifurcated (2DB) supersonic inlet, previously utilized in the NASA High Speed Research program will also be used here for the controls design studies.

Closed loop control of the shock position downstream of the inlet throat is primarily accomplished by adjusting the bypass door exit area to bleed air out of the inlet. An upstream movement of the shock position will cause the controller to open the bypass door, and vice versa. The center body for an axisymmetric inlet or the forward ramps for a square shaped inlet can also translate to control the shock, but these actuation systems have much slower response times and are often scheduled open or closed loop. In this control design, the inlet operating point will be at cruise (M~2.35) and the control design will be examined at this operating point, without control of the slower inlet translating center body or the ramps.

For a linear control design, the representative TFs are obtained by applying frequency sweeps to the LAPIN model to generate TF for the variables of interest for both the disturbances and the control variables. The disturbance TFs were fitted with poles and zeros by using MATLAB (The MathWorks, Inc.) System ID. The TF for the control variables were fitted by hand, because even though System ID does a good job fitting the magnitude, that was not the case for the phases, which are very important for controls design. The accuracy of the sinusoidal sweeps to generate accurate TFs was always verified by examining the coherence.

A. Inlet Plant Transfer Functions

The overall inlet feedback control system for this study consists of the inlet bypass door actuator, the actuator position (corresponding to the bypass door area opening) to the shock position response, and the feedback controller that controls the actuator to position the shock. The plant TF for the inlet system will then be a product of the actuator TF and the actuator position to the shock response TF. Disturbances come in at the output of this control system, at the shock position, similar to the feedback control diagram shown in Figure 2. The center body for an axisymmetric inlet or the ramps for a two-dimensional type inlet are also controlled either open or closed loop and this control also effects the shock position. However, even closed loop control for these geometries is relatively slow compared to the bypass door actuation response. Therefore, centerbody or ramp control for the shock is not anticipated to significantly add to the overall disturbance rejection of the system, especially at higher frequencies where it is most important, and thus this type of control will not be included in this study.

Using these sinusoidal sweeps with the LAPIN model, the bypass door to shock position TF was derived as

$$G_{BS}(s) = \frac{3.325K_{cr}(s/653+1)(s/2513+1)}{(s/118+1)(s^2/911^2+1.5s/911+1)(s^2/3142^2+1.1s/3142+1)(s^2/3330^2+1.3s/3330+1)} * \frac{1}{(s^2/3519^2+1.3s/3519+1)(s^2/3707^2+1.3s/3707+1)} \quad (6)$$

where K_{cr} is a geometric scale property of the cowl lip radius utilized in the LAPIN model.

A Moog, Inc., valve was used for the bypass door actuator, based on past experimental setups utilized for the 2DB supersonic inlet. This valve with the vendor controller (inner loop) and the feedback controller designed in this development (outer loop) is shown in Figure 5. The transfer function of the valve and the various gains shown for the valve feedback are taken from vendor literature. The inner valve feedback control design is set by the vendor and cannot be changed. The outer loop feedback controller is designed here to provide a control bandwidth of about 175 Hz, again based on vendor specifications for the valve. The rest of the controller design (i.e., the outer loop shown in Figure 5) is used to provide high disturbance attenuation of 20 dB or greater at the mid-frequency range and a phase and gain margin of greater than 60° and 10 dB respectively. This design will not be detailed here, but it follows along the same design procedures discussed in the previous section (Ref. 7) and the design of the shock controller that will be discussed later. The overall input/output TF of the valve and its feedback controller is approximated as

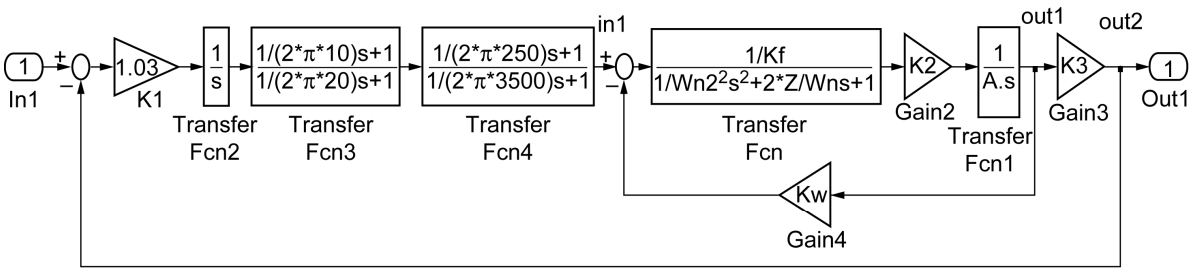

Figure 5.—Feedback control design diagram of the Moog valve position.

$$G_A(s) = \frac{(s/63+1)}{(s/60+1)(s^2/1136^2 + 0.8s/1136+1)(s^2/4753^2 + 0.6s/4753+1)} \tag{7}$$

This approximation is computed to match the actual TF (both magnitude and phase) of the valve feedback control system from low frequency up to a little over the cross-over frequency of its CLG.

B. Inlet Disturbance Transfer Functions

The main objective of the inlet shock control system is to maintain the shock at a desired position downstream of the inlet throat in the presence of upstream disturbances (i.e., atmospheric, aeroservoelastic, yaw, and angle of attack) and downstream disturbances (coming from the engine). For the upstream disturbances, how the inlet itself propagates these disturbances in terms of Mach number, static pressure and static temperature to effect the shock position needs to be taken into account. For the control analysis presented in this paper, only the atmospheric disturbances will be included. Thus, the atmospheric disturbance models for these flow quantities are also needed in this analysis.

Perturbing the LAPIN model with sinusoidal sweeps and using MATLAB System ID to estimate the TF of the inlet disturbances, the static pressure to shock position TF is computed as

$$G_{PS}(s) = \frac{1.55s^5 - 2.08e4s^4 + 5.37e7s^3 - 8.19e10s^2 + 2.16e14s - 8.75e14}{s^6 + 3.09e3s^5 + 1.07e7s^4 + 1.78e10s^3 + 1.66e13s^2 + 8.62e15s + 6.86e17} \tag{8}$$

As mentioned before, the phase of these disturbance TFs, which would be associated with the time delay as a function of frequency that it would take for a disturbance to be felt at the shock, was not matched with MATLAB System ID and it was offset by 360°, as a phase lead. Thus, it is assumed that a phase lead would be worst case compared to the actual time delay of the disturbances. But in the future these disturbance TFs will be more accurately fitted to incorporate better accuracy for the phase delay as well. Similarly, the static temperature to shock TF was computed as

$$G_{TS}(s) = \frac{\begin{array}{c} -4.89s^7 + 1.78e4s^6 - 5.69e7s^5 + 1.28e11s^4 \\ -2.20e14s^3 + 1.12e17s^2 - 2.93e20s - 6.26e \end{array}}{\begin{array}{c} s^8 + 3.87e3s^7 + 1.51e7s^6 + 3.46e10s^5 + 5.69e13s^4 \\ +7.02e16s^3 + 4.97e19s^2 + 2.65e22s + 3.47e24 \end{array}} \tag{9}$$

The Mach number to shock TF was computed as

$$G_{MS}(s) = \frac{4.88e2s^6 - 3.24e6s^5 + 9.16e9s^4 - 1.01e13s^3}{s^7 + 3.12e3s^6 + 1.42e7s^5 + 2.16e10s^4 + 3.88e13s^3} \\ \frac{+ 2.69e16s^2 + 1.52e19s + 4.69e21}{+ 2.23e16s^2 + 1.31e19s + 1.21e21} \tag{10}$$

C. Atmospheric Disturbances

Derivations for atmospheric disturbance spectral densities for variations in acoustic velocity, temperature, and pressure are shown in Reference 9. In this Reference, atmospheric disturbance models were created by scaling an existing model and by fitting these atmospheric models, which are fractional order, with a product of first order poles and zeros. Then time domain atmospheric disturbances can be obtained by forming a combination of unit magnitude sinusoids, distributed in frequency starting from low sub hertz frequencies up to about 200 Hz (approximately the bandwidth limitation for the type of actuators used for bypass doors), which are used as inputs to the TFs representing these atmospheric disturbances.

Thus, atmospheric disturbance TF for the longitudinal acoustic velocity is expressed as (Ref. 9)

$$G_{LA}(s) = \frac{8.74(s/9.2+1)(s/55.0+1)(s/335.5+1)}{(s/1.46+1)(s/30.1+1)(s/85.7+1)(s/1593.1+1)} \tag{11}$$

where ε stands for the eddy dissipation rate, which has a worst case value of 8.6×10^{-5} (m^2/s^3) based on data collected at altitudes of 25 to 40 k ft; *L* stands for the integral length scale with a typical value of 762 m, which is related to outer length scale that signifies the length of the atmospheric turbulence patch (Ref. 9). The eddy dissipation rate has values that increase in magnitude with decreasing altitude below 25 k ft, and it is orders of magnitude larger near ground level. For this study, supersonic operation implies that the shock control will be needed only at relatively high altitudes. The atmospheric temperature disturbance TF is expressed as (Ref. 9)

$$G_T(s) = \frac{41.75(s/33.0+1)(s/45.6+1)(s/602.4+1)}{(s/1.1+1)(s/25.1+1)(s/109.8+1)(s/816.3+1)} \tag{12}$$

Temperature fluctuations will cause acoustic velocity disturbances through the speed of sound change, and this velocity disturbance due to temperature is expressed as

$$G_{TA}(s) = \frac{M\gamma R}{a_o}\frac{20.88(s/33.0+1)(s/45.6+1)(s/602.4+1)}{(s/1.1+1)(s/25.1+1)(s/109.8+1)(s/816.3+1)} \tag{13}$$

where *M* signifies the Mach number, γ is the ratio of specific heats, *R* is the universal gas constant in units of (N*m)/(kg*°K), and a_o is the local speed of sound. Close examination of Equation (13) will show that acoustic disturbances due to temperature fluctuations are considerably larger than those due to pure acoustic velocity fluctuations, Equation (11). The atmospheric pressure disturbance TF is expressed as (Ref. 9)

$$G_P(s) = \frac{37.96(s/33.0+1)(s/45.6+1)(s/602.4+1)}{(s/1.1+1)(s/25.1+1)(s/109.8+1)(s/816.3+1)} \tag{14}$$

These atmospheric TFs have corresponding units of m/s (Eqs. (11) and (13)), °K (Eq. (12)), and Pa (Eq. (14)). The input to these TFs are unitless sinusoids of unit amplitude, uniformly distributed in frequency.

IV. Inlet Shock Position Control Design

Having derived the inlet linear plant model for shock position control at cruise and the bypass door actuation system TF as well as the atmospheric disturbance models and inlet disturbance TFs, the control design can begin. Of course, the cruise operating point is just one point in the plant model and the plant model can differ for different operating points. However, the Supersonics Project has not yet baselined an inlet design and also, the objective of this control design is to demonstrate a design methodology, rather than an encompassing control design for the entire operating envelope.

The approach for the feedback control design has been discussed briefly in Section II and in more detail in Reference 7. The approach that has been taken for this control design is to maximize disturbance rejection based on the actuation system bandwidth capability listed in Vendor's specifications, as discuss in Section III, while providing sufficient stability margins (i.e., about 60° phase margin or greater and at least 10 dB gain margin). The next step is to conduct simulations and analysis to understand how this control design handles these disturbances (for now just atmospheric disturbances). For the shock position control or in general, this design approach allows the designer to maximize the performance of the control system and it also provides for real justification to ask for additional hardware capability in case the design doesn't meet the prescribed requirements.

A block diagram of the inlet shock position feedback control system via bypass door control with the atmospheric disturbances is shown in Figure 6. In the actual shock control system, the actuator feedback control (Fig. 5) takes the place of $G_A(s)$. The command schedule block (Cmnd Sch) in this figure is a control schedule for the actuator, which is utilized to move the bypass door to the desired position required to initialize the shock control system and it's a constant in this study.

As discussed before, the first step of the loop shaping control design methodology (Ref. 7) is to decide on the control bandwidth (i.e., the cross-over frequency) based on the speed or bandwidth of the actuation system. Since the Moog valve was used before for actuating the bypass door, and its specification called for a bandwidth up to about 175 Hz, the same bandwidth was selected for the actuator feedback control system. Disturbance attenuation for the actuator position, for disturbances coming from the vehicle structural vibration modes, was also considered important for this design. Also since this control design is multi-loop, disturbance rejection capability of the actuator position control loop would be expected to contribute to the overall shock position disturbance rejection performance. The details of the actuator feedback control design shown in Figure 5 will not be discussed in this paper, but are similar to the design that will be described for the shock position feedback control system. Based on this bandwidth of the actuator feedback control system, the shock position feedback control system bandwidth

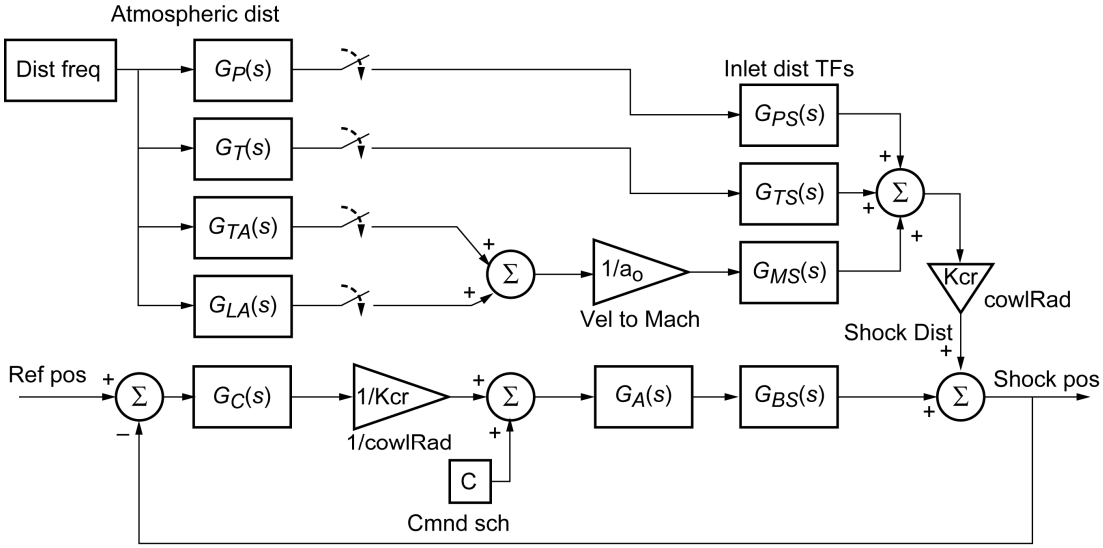

Figure 6.—Feedback control diagram of inlet shock position system via bypass door actuation.

was chosen to be about 145 Hz. Normally, significant separation would be designed for these control bandwidths to avoid coupling, but such a design would significantly compromise disturbance attenuation. However, designing the controller with a hybrid or composite dominant natural frequency will help to mediate (to some degree) the coupling problem for the outer loop of the shock control feedback. Still, in the final control system design, this bandwidth may need to be lowered if the speed of the outer loop causes the valve position control loop to be overdriven. Thus, the approach is to design the control bandwidth as high as possible, without taking into consideration the disturbance frequencies, in order to enable maximizing disturbance attenuation. More on this subject will be discussed later.

After determining the control system bandwidth, the CLG can be shaped to meet these specifications. For a mid-frequency gain of 20 dB (for disturbance rejection) and for the CLG to cross-over at 145 Hz, a pole needs to be placed one decade below this frequency, at 14.5 Hz (remember the gain slope due to a pole is –1 or –20 dB/decade). Next, select the frequency where the low frequency zero will be placed. The main purpose of the low frequency zero is to preserve the gain of the CLG at the mid-frequency range for disturbance attenuation and to boost the phase for better phase margin at the cross-over frequency. But the low frequency zero of the CLG will also influence the response time, especially the settling time (Ref. 7). For the phase boost, it is advantageous to place the zero lower in frequency, and for the settling time it is beneficial is to place the zero at higher frequency. So some compromise is in order. With no hard requirement for the settling time, the frequency of the zero was placed at 5 Hz. Also, for zero steady state error, a pole needs to be placed at the origin. For disturbance attenuation, a mid-frequency gain of 20 dB is chosen for the CLG, which maximizes the mid-frequency gain for maximum disturbance attenuation. Actually, it is possible to obtain a little more mid-frequency gain with a little more complicated design (Ref. 7). Based on the disturbance attenuation design of 20 dB at the mid-frequency range (starting at 5 Hz) and with only the pole at zero influencing the magnitude of the CLG up to that point, the gain of the CLG at the frequency of the zero can be calculated as

$$\left|L(j\omega)\right| = \left|\frac{K_L}{s}\right|_{\omega=2\pi(5)} = 20dB \tag{15}$$

where K_L is the proportional gain of the CLG, L. Based on Equation (15), this gain can be calculated as $K_L = 2\pi(5)10^{20/20} = 310$ (i.e., the antilog based on $20\log_{10}(x)$). In actuality, the gain will break 3 dB above at the frequency of the zero and 3 dB below at the frequency of the pole. In general the proportional gain of the CLG is

$$K_L = \omega_z 10^{L_{mfr}/20} \tag{16}$$

where ω_z is the frequency where the zero is placed and L_{mfg} is the gain of the CLG desired or specified at the mid-frequency range. This completes the design of the CLG as

$$L(s) = 310\frac{(s/(2\pi 5)+1)}{s(s/(2\pi 14.5)+1)} \tag{17}$$

Barring the fact that the shock controller in this design is a multi-loop controller with almost overlapping loop bandwidths, a single loop control system with this CLG design will have a phase margin of $\phi M = 180 - 90 + 90 - 90 = 90°$ (more than enough) and an infinite gain margin. A bode plot of this design is shown in Figure 7.

In order for the CLG of the feedback control system to approximate the design of Equation (17), it means that the controller times the plant TFs will also need to equate to this CLG as

$$L(s) = G_C(s)G_A(s)G_{BS}(s) \tag{18}$$

Therefore, using Equations (7), (6), and (17) (see also Fig. 6), the controller TF can be calculated as

$$G_C(s) = \frac{L(s)}{G_A(s)G_{BS}(s)} \tag{19}$$

Or in terms of magnitude in dB scale, where it would be desirable to display $G_C(s)$ in order to fit the approximation with poles and zeros

$$\left|G_C(s)\right| = 20\log_{10}\left|L(s)\right| - 20\log_{10}\left|G_A(s)G_{BS}(s)\right| \tag{20}$$

And the phase can be computed as

$$\phi(G_C(s)) = \phi(L(s)) - \phi(G_A(s)G_{BS}(s)) \tag{21}$$

Figure 8 shows the calculation of the controller TF $G_C(s)$ and its fitting with poles and zeros. This fitting was done by hand, which resulted in the control TF as

$$\begin{aligned} G_C(s) = {} & \frac{310(s/2\pi5+1)(s/2\pi18.8+1)}{s(s/2\pi14.5+1)(s/2\pi104+1)} \\ & \frac{(s^2/(2\pi145)^2 + 0.98s/2\pi145+1)(s^2/(2\pi250)^2 + 1.3s/2\pi250+1)}{(s^2/(2\pi5000)^2 + 1.4s/2\pi5000+1)(s^2/(2\pi5500)^2 + 1.4s/2\pi5500+1)} \\ & \frac{(s^2/(2\pi350)^2 + 1.36s/2\pi350+1)(s^2/(2\pi450)^2 + 1.0s/2\pi450+1)}{(s^2/(2\pi6000)^2 + 1.4s/2\pi6000+1)(s^2/(2\pi6500)^2 + 1.4s/2\pi6500+1)} \\ & \frac{(s^2/(2\pi550)^2 + 1.0s/2\pi550+1)(s^2/(2\pi650)^2 + 0.60s/2\pi650+1)}{(s^2/(2\pi7000)^2 + 1.4s/2\pi7000+1)(s^2/(2\pi7500)^2 + 1.4s/2\pi7500+1)} \end{aligned} \tag{22}$$

The high frequency poles in Equation (22) (those in the 1000's of Hz) are inserted in order to make the controller TF proper without impacting the phase at the frequency range of interest for the fit, but not too high in frequency to significantly slow down the simulation. Figure 9 shows how the design CLG with the computed controller TF matches the desired CLG of Equation (17) (Fig. 7) when inserted into the shock control feedback system of Figure 6 with the actual valve feedback controller. As can be seen, the actual phase of the control system design deviates somewhat at the cross-over and beyond, but there is still plenty of phase margin. Also, the gain after the cross-over needs to keep on decreasing (especially near the cross-over), which it does, but it is not fully shown in this figure.

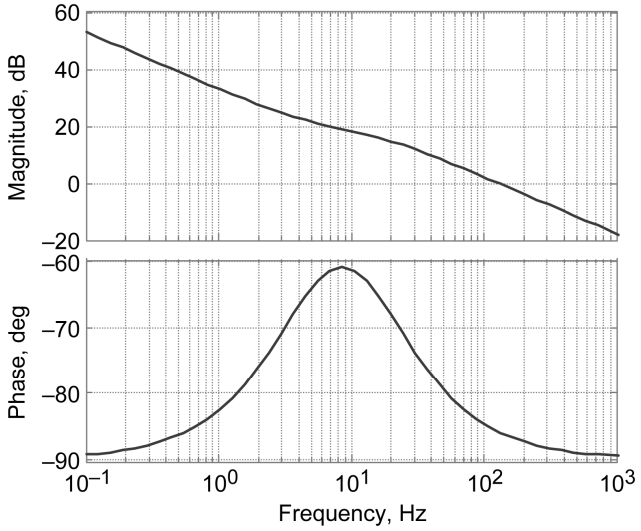

Figure 7.—Bode plot of the CLG design of Equation (17).

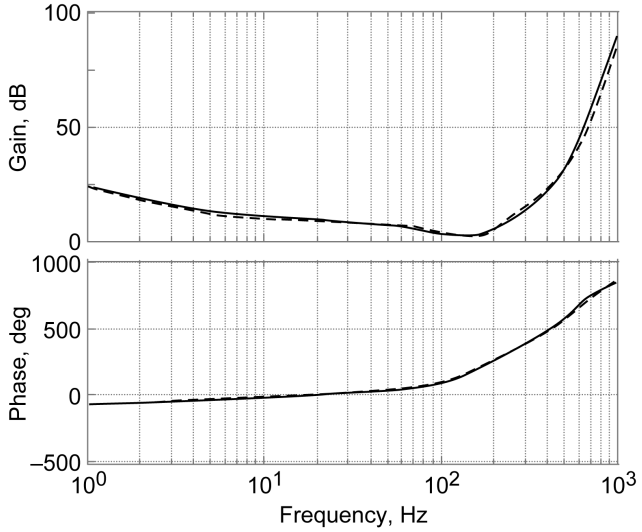

Figure 8.—Calculated Controller TF based on Equations (19) and (20) and its pole/zero fit.

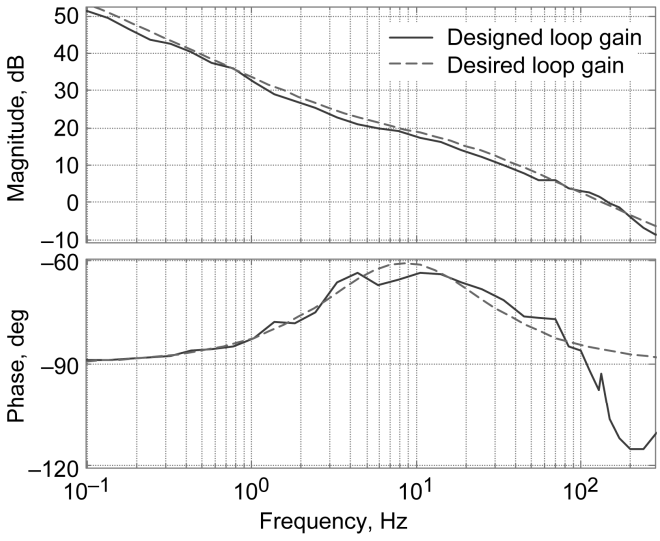

Figure 9.—Bode plot of the desired CLG design of Equation (17) and the CLG of actual feedback control system.

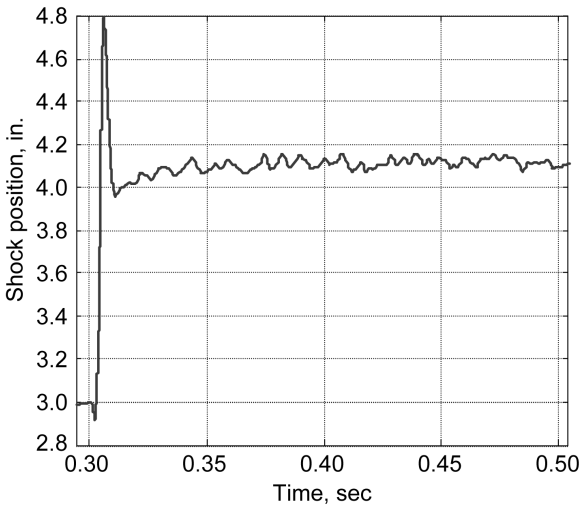

Figure 10.—Shock position response of the controller design based on Equation (22).

Figure 10 shows a step response starting from zero initial conditions for the shock response. It turns out that the valve position is overdriven in this design, generating relatively large excursions (not shown) as evident by the chopping response, because of the tightly coupled control bandwidths of the multi-loop controllers. In terms of the large overshoot in this design, two points can be made. One, the shock position reference will not be commanded in a step fashion, so there is nothing that will move the shock instantaneously. Thus, that will not be a problem as long as the system is stable. Secondly, under an ordinary design, this much overshoot will render the control system oscillatory and virtually unstable. However, as discussed before, the composite natural response in this design, with the low frequency zero dominating the response after the initial response takes place, has a stabilizing effect on the control system by changing the control system response from second order to a first order type. It is beneficial to have a fast initial response, indicative of a high bandwidth control design, because such a design allows for a high disturbance attenuation design.

The oscillations in the response shown in Figure 10, due to overdriving the valve position control, can be improved by decreasing the controller gain in Equation (22) until a satisfactory response is obtained that includes the valve position. By decreasing the controller gain, the bandwidth will decrease, but disturbance attenuation will decrease proportionally as well. Based on that, the controller gain in Equation (22) was decreased to 100, which equates to approximately 10 dB reduction in gain. Thus, roughly from Figure 9, subtracting 10 dB from the gain will cause the CLG to cross-over at about 35 Hz. The step response of the shock control system with this reduction in the controller gain is shown in Figure 11.

Once the desired cross-over frequency or bandwidth (that sufficiently reduces coupling) in this multi-loop control system is found, the proper design procedure would be to repeat the whole controller design process in order to maximize disturbance rejection. Again, the frequencies of the disturbances are not taken into account in the design of the bandwidth of the control system. The reason is that if the highest possible control bandwidth is designed, and if it turns out that this is not good enough for disturbance rejection (in terms of let's say of the command tracking performance or control margin reduction), the option left is to request more capability from the hardware designs, such as actuation speeds. Repeating the control design process, with the newly found bandwidth, will not be done here and for the studies that follow a controller gain of 100 is used.

Atmospheric disturbances were applied utilizing Equations (11) to (14) with unit amplitude sinusoidal inputs distributed from very low frequencies up to 200 Hz as shown in the feedback control diagram of Figure 6. A time domain slice of these disturbances is shown in Figure 12. A control disturbance response was assumed with worst case atmospheric disturbance conditions at high altitudes as those shown in Figure 12 with an eddy dissipation rate $\varepsilon=8.6\times10^{-5}$, with a longitudinal acoustic wave velocity

disturbance along the axis of the inlet accompanied by a temperature fluctuation that also produces acoustic wave velocity disturbances, together with a pressure fluctuation. The combined disturbances influencing the shock position, and the feedback control responses are shown in Figure 13. It can be seen from the control response that this feedback control system design does a good job attenuating anticipated worst case atmospheric disturbances, down to about 0.15 in. peak-to-peak.

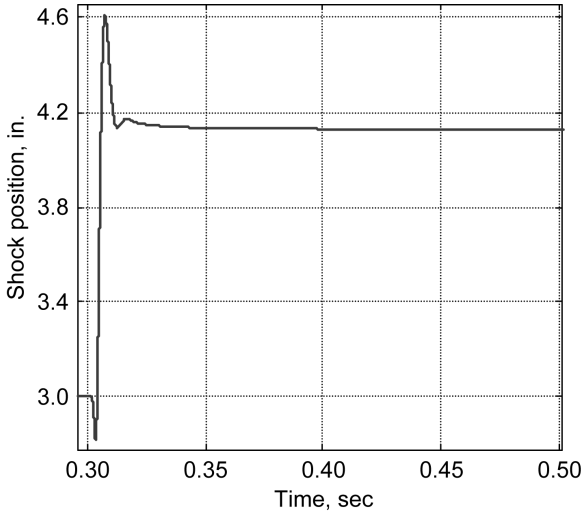

Figure 11.—Shock position response of the controller design with a gain of 100.

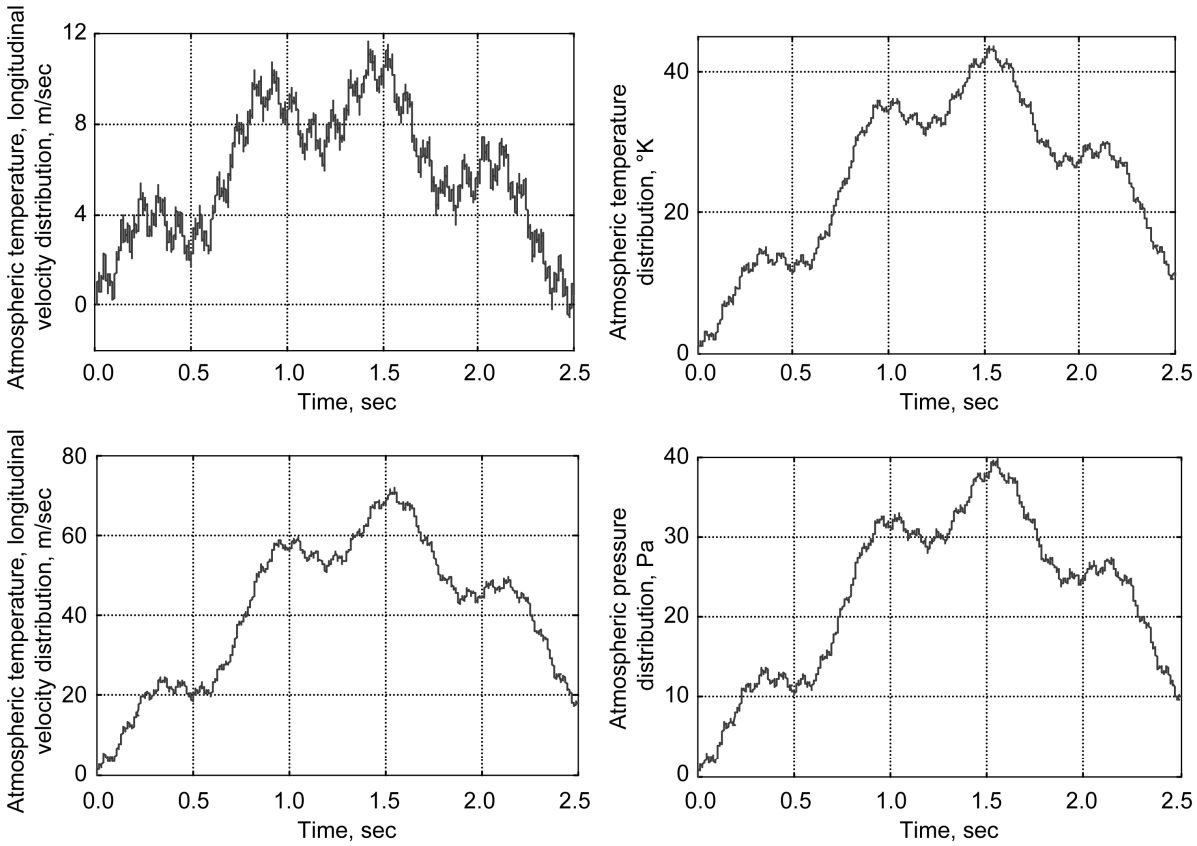

Figure 12.—Atmospheric disturbances of Equations (11) to (14).

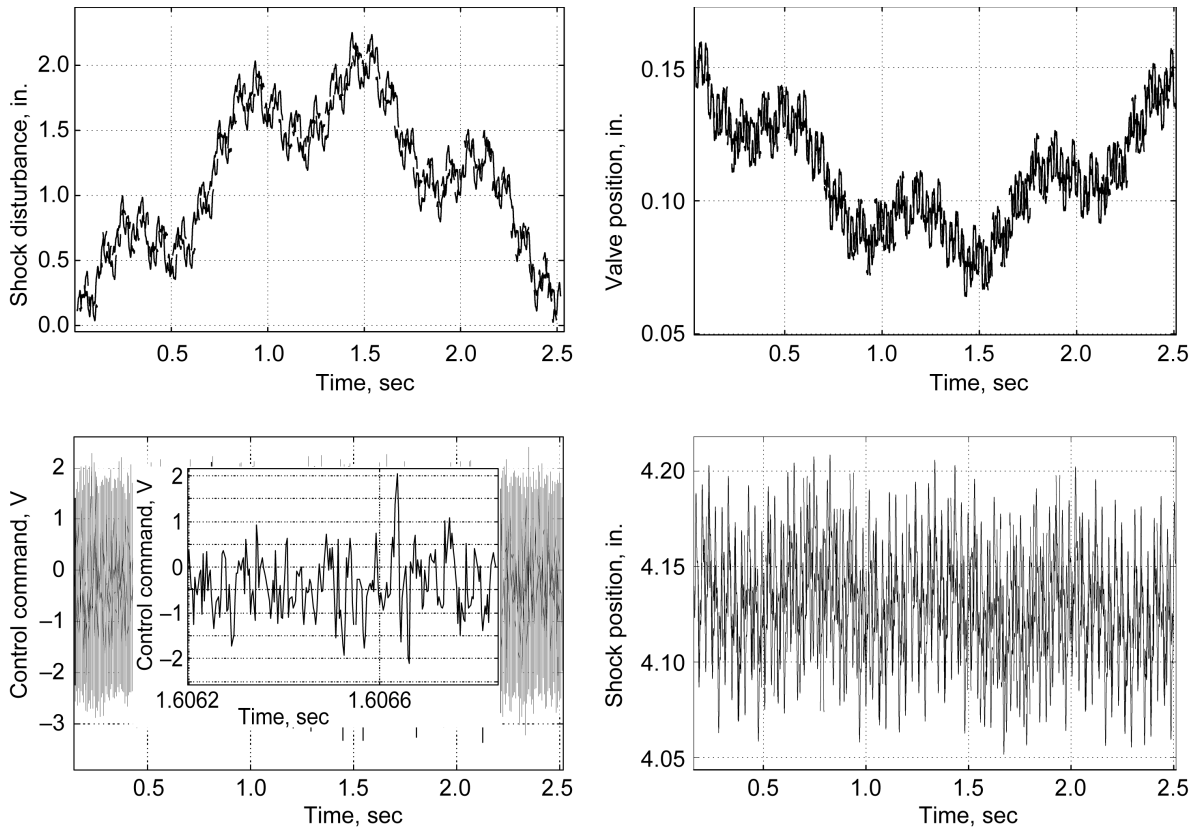

Figure 13.—Shock disturbance, control command, valve position, and shock position response due to atmospheric disturbances of Equations (11) to (14).

Checking the actuation rates of the valve position (not shown in detail in Fig. 13), it turns out that the actuation rates are well below that corresponding to the valves 175 Hz bandwidth, which satisfies the design. The low actuation rates are the result of the atmospheric disturbances whose spectral densities decrease with frequency as well as the volume of the inlet which also attenuates these disturbances. Therefore, based only on these results and if needed, the bandwidth of the actuator position controller can be increased with a corresponding increase on the shock position controller bandwidth without violating the actuator bandwidth limit. However, in order to increase the bandwidth of the valve controller outer loop, the inner loop design (Fig. 5) would also need to be taken into account.

A single frequency disturbance of amplitude of one peak-to-peak was applied at a 10 Hz frequency to check the mid-frequency disturbance attenuation of this design as shown in Figure 14. The disturbance attenuation shown with the shock position is approximately 20 dB. This disturbance attenuation is achieved despite the gain reduction discussed before of about 10 dB, which was expected to reduce mid-frequency disturbance attenuation by 10 dB (i.e., reduced down from the original design of 20 dB). The reason is that the shock position control loop is working in concert with the actuator control loop to enhance disturbance rejection.

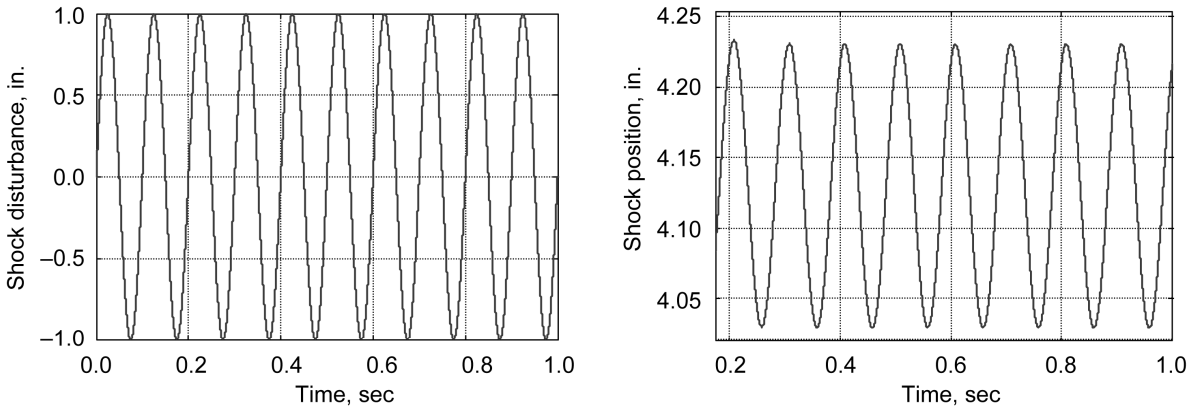

Figure 14.—Shock disturbance at mid-frequency (10 Hz) and shock position response.

V. Conclusion

In this paper a systematic inlet shock position control system design based on feedback loop shaping was demonstrated with emphasis on disturbance rejection. Results presented with atmospheric disturbances show that the shock position control is able to sufficiently reject these disturbances. More work remains to be done to also add inlet upstream flow field disturbances generated from the vehicle aeroservoelastic modes, also disturbances from the vehicle pitch and yaw maneuvers, as well as downstream disturbances coming from the rest of the propulsion system. In addition, linear models of the inlet need to be generated at other flight conditions, from transonic all the way to cruise, and similar control design and analysis would need to be conducted. Finally, the control design would need to be applied to the nonlinear inlet model as well to the integrated propulsion system, and finally to the aeropropulsoservoelastic system of the integrated vehicle. However, so far it is encouraging to see that the inlet shock position control system has no trouble attenuating expected atmospheric disturbances. If this trend of tight shock position control can be maintained throughout the operating envelope and disturbances, it could allow a decrease in the shock position margin and thus an increase in the propulsion efficiency.

References

1. Cole, G.L., “Atmospheric Effects on Inlets for Supersonic Cruise Aircraft,” NASA TM X–73647, AIAA–77–874, Thirteenth Propulsion Conference, Jul. 11–13, 1977.
2. Chang, J., “Observers Design for Shock Position of Supersonic Inlet Based on Equilibrium Manifold,” AIAA, 42nd Joint Propulsion Conference, Jul. 9–12, 2006.
3. Ahsun, U., “Design of a Near-Isentropic Supersonic Inlet Using Active Control,” Journal of Propulsion and Power, Vol. 21 No. 2, Mar.–Apr. 2005.
4. MacMartin, D.G., “Dynamics and Control of Shock Motion in a Near-Isentropic Inlet,” Journal of Aircraft, Vol. 41, No. 4, July-August, 2004.
5. Yarng, J.B., “Optimal Control of Supersonic Inlet/Engine Combination,” Journal of Guidance Control and Dynamics, Vol. 11, No. 2, Mar.–Apr. 1988.
6. Lehtinen, B., “Application of Quadratic Optimization to Supersonic Inlet Control,” NASA TM X–67905, Fifth Congress of the International Federation of Automatic Control,” June 12–17, 1972.
7. Kopasakis, G., “Feedback Control Systems Loop Shaping Design With Practical Considerations,” NASA/TM—2007-215007, Sept. 2007.
8. Varner, M.O., Martindale, W.J., Phares, K.R., Kneile, K.R., Adams, J.C., “Large Perturbation Flow Field Analysis and Simulation for Supersonic Inlets Final Report,” NASA CR–174676.
9. Kopasakis, G., “Atmospheric Turbulence Modeling for Aero Vehicles—Fractional Order Fits,” NASA TM submitted for publication.

REPORT DOCUMENTATION PAGE	Form Approved OMB No. 0704-0188

1. REPORT DATE *(DD-MM-YYYY)*	2. REPORT TYPE	3. DATES COVERED *(From - To)*
01-02-2010	Technical Memorandum	

4. TITLE AND SUBTITLE
Shock Positioning Controls Design for a Supersonic Inlet

5a. CONTRACT NUMBER

5b. GRANT NUMBER

5c. PROGRAM ELEMENT NUMBER

6. AUTHOR(S)
Kopasakis, George; Connolly, Joseph, W.

5d. PROJECT NUMBER

5e. TASK NUMBER

5f. WORK UNIT NUMBER
WBS 984754.02.07.03.20.02

7. PERFORMING ORGANIZATION NAME(S) AND ADDRESS(ES)
National Aeronautics and Space Administration
John H. Glenn Research Center at Lewis Field
Cleveland, Ohio 44135-3191

8. PERFORMING ORGANIZATION REPORT NUMBER
E-17122

9. SPONSORING/MONITORING AGENCY NAME(S) AND ADDRESS(ES)
National Aeronautics and Space Administration
Washington, DC 20546-0001

10. SPONSORING/MONITOR'S ACRONYM(S)
NASA

11. SPONSORING/MONITORING REPORT NUMBER
NASA/TM-2010-216074

12. DISTRIBUTION/AVAILABILITY STATEMENT
Unclassified-Unlimited
Subject Category: 08
Available electronically at http://gltrs.grc.nasa.gov
This publication is available from the NASA Center for AeroSpace Information, 443-757-5802

13. SUPPLEMENTARY NOTES

14. ABSTRACT
Under the NASA Fundamental Aeronautics Program, the Supersonics Project is working to overcome the obstacles to supersonic commercial flight. The supersonic inlet design that is utilized to efficiently compress the incoming air and deliver it to the engine has many design challenges. Among those challenges is the shock positioning of internal compression inlets, which requires active control in order to maintain performance and to prevent inlet unstarts due to upstream (freestream) and downstream (engine) disturbances. In this paper a novel feedback control technique is presented, which emphasizes disturbance attenuation among other control performance criteria, while it ties the speed of the actuation system(s) to the design of the controller. In this design, the desired performance specifications for the overall control system are used to design the closed loop gain of the feedback controller and then, knowing the transfer function of the plant, the controller is calculated to achieve this performance. The innovation is that this design procedure is methodical and allows maximization of the performance of the designed control system with respect to actuator rates, while the stability of the calculated controller is guaranteed.

15. SUBJECT TERMS
Supersonic inlet control; Inlet control; Inlet feedback control; Atmospheric disturbances; Atmospheric turbulence

16. SECURITY CLASSIFICATION OF:			17. LIMITATION OF ABSTRACT	18. NUMBER OF PAGES	19a. NAME OF RESPONSIBLE PERSON
a. REPORT	b. ABSTRACT	c. THIS PAGE			STI Help Desk (email:help@sti.nasa.gov)
U	U	U	UU	22	19b. TELEPHONE NUMBER *(include area code)* 443-757-5802